Molecular Structure of Polystyrene at Air/Polymer and Solid/Polymer Interfaces

K. S. Gautam, A. D. Schwab, and A. Dhinojwala*
The University of Akron, Akron, Ohio 44325

D. Zhang, S. M. Dougal, and M. S. Yeganeh†
ExxonMobil Corporate Strategic Research Laboratories, Annandale, New Jersey 08801
(Received 12 May 2000)

IR-visible sum-frequency generation (SFG) spectroscopy has been used in a total internal reflection geometry to study the molecular structure of polystyrene (PS) at PS/sapphire and PS/air interfaces, simultaneously. The symmetric vibrational modes of the phenyl rings dominate the SFG spectra at the PS/air interface as compared to the antisymmetric vibrational modes at the PS/sapphire interface. This indicates approximately parallel orientation of the phenyl rings at the PS/air interface while nearly perpendicular orientation at the PS/sapphire interface, with respect to the surface normal.

PACS numbers: 61.41.+e

The molecular structure of polymer layers near solid surfaces has important technical implications in materials science [1]. The stability of thin polymeric films, the tenacity of adhesives to bond, and the strength of polymer-polymer interfaces are a few examples where the knowledge of polymer-solid interfaces is critical. Past experimental and theoretical studies have focused on understanding segregation of chain ends [2], conformation of polymer chains [3], and segregation of polymers of different architecture next to solid surfaces [4,5]. However, the organization on a more local scale, for example, of repeat units or sidegroups of polymer chains at interfaces, is poorly understood. Recent theoretical calculations suggest that the side chains of substituted polymers are preferentially present near a noninteractive wall [6]. The density of the sidegroups is influenced by the wall-polymer and polymer-polymer interaction energies. One expects that the local density and orientation of sidegroups near solid surfaces can be quite different from that at a more hydrophobic air/vacuum interface.

In this Letter, we report for the first time, a direct experimental measurement of the surface structure of a polymer layer at both solid and air interfaces. We have developed a novel experimental protocol to nondestructively study the surface structure of hidden (solid/polymer) and free (air/polymer) interfaces using sum-frequency vibrational spectroscopy (SFG) in total internal reflection geometry. SFG involves mixing a visible high intensity laser beam of frequency ω_1, with a tunable infrared wavelength source of frequency ω_2. According to dipole approximation, generation of a SFG photon [at $(\omega_1 + \omega_2)$] is forbidden in the centrosymmetric bulk and is nonzero at interfaces where inversion symmetry is broken [7]. The SFG is resonantly enhanced when ω_2 overlaps with the resonant frequency of a molecular vibrational mode that is both infrared and Raman active. The intensity, polarization, and resonance frequency of the SFG signal yield chemical and orientational information of molecules at interfaces. The SFG output is also enhanced by 1 to 2 orders of magnitude when the incidence angles of the input beams are close to the critical angle for total internal reflection (explained by higher Fresnel coefficients of the reflected SFG signal near critical angles) [8]. We have used this enhancement in SFG signals at critical angles to independently probe the structure at air/polystyrene (PS) and solid/PS interfaces.

SFG experiments were performed at the ExxonMobil SFG II system and involved overlapping visible (532 nm, 7 ns duration pulse) and tunable infrared (1300–3800 cm^{-1}, 7 ns duration pulse) beams at the polymer surface. The visible beam was generated by a frequency-doubled Nd-YAG laser and the tunable infrared beam by stimulated Raman scattering of a tunable dye laser beam in a hydrogen Raman cell. The infrared beam has a wave number resolution of less than 1 cm^{-1}. The details of the experimental setup have been published elsewhere [9]. Uniform films of PS ($M_w = 200\,000$ g mol^{-1}, atactic and monodisperse), 160 nm thick, were prepared on sapphire prisms by spin coating using a 2 wt % solution of PS in toluene. The PS films were annealed at 110 °C ($T_g = 105$ °C as determined by differential scanning calorimetry) in a vacuum oven for 4–5 h. The SFG spectra reported here were taken at 24 °C. The critical angle, based on refractive indices of air, PS, and sapphire, is 36° for PS/air and 64° for the PS/sapphire interface. The phenyl sidegroups in PS exhibit five vibrational modes composed of C-H aromatic stretches, which are both Raman and infrared active. These five modes are believed to have resonance frequencies at 3084, 3069, 3057, 3036, and 3024 cm^{-1} corresponding to the ν_{20a}, ν_2, ν_{7b}, ν_{7a}, and ν_{20b} vibrational modes, respectively [10,11].

Figure 1 shows the incident angle dependence of the SFG intensity (Issp, s-polarized output, s-polarized visible input, and p-polarized infrared input) at two infrared frequencies, 3028 and 3067 cm^{-1}. These two frequencies were chosen because the strongest SFG signals were observed at 3028 and 3067 cm^{-1} for PS/sapphire and PS/air interfaces, respectively. It is clear that the SFG intensity is enhanced near both of the predicted critical

 0031-9007/00/85(18)/3854(4)$15.00

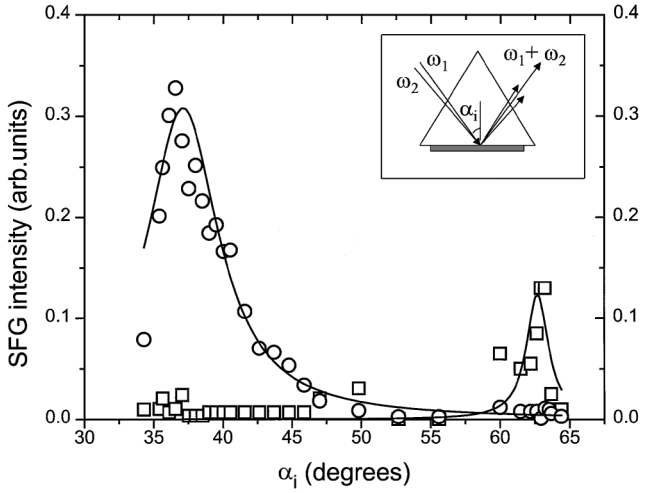

FIG. 1. The SFG intensity Issp as a function of incident angle α_i for two wave numbers (ω_2), 3027 cm^{-1} (squares) and 3067 cm^{-1} (circles). The data represented by circles are scaled by a factor of 5. The solid line is a visual guide to illustrate the spectral trends.

angles corresponding to the PS/air (36°) and PS/sapphire (64°) interfaces. The SFG signals at the PS/sapphire interfaces are an order of magnitude smaller than the PS/air interface and have been scaled by a factor of 5 in order to compare them with the values obtained for the PS/air interface. This indicates that it would be difficult to isolate the signal for the PS/sapphire interface from the PS/air signal using an external reflection geometry. Surprisingly, the peak at 3067 cm^{-1} dominates the PS/air spectra in comparison with the peak at 3028 cm^{-1} for the PS/sapphire interface. A complete analysis of the angular dependence of the SFG intensity will be presented elsewhere.

To obtain complete spectral information of both the interfaces, SFG spectra of the PS/air and PS/sapphire interfaces were collected as a function of infrared frequency, ω_2, by fixing $\alpha_i = 36°$ (Fig. 2) and $\alpha_i = 64°$ (Fig. 3), respectively. Spectra were obtained using two polarization combinations, Issp and Ippp (p-polarized output, p-polarized visible input, p-polarized infrared input). SFG spectra for both PS/air and PS/sapphire interfaces contain peaks between 3000–3100 cm^{-1}, corresponding to aromatic C-H stretching vibrations. A sharp resonance at 3069 cm^{-1} corresponding to the ν_2 vibrational mode dominates the Ippp and Issp spectra for PS/air interface. In comparison to the PS/air spectra, the PS/sapphire spectra are notably different in the aromatic stretch region. The Ippp and Issp spectra for PS/sapphire interface show three prominent resonance features at 3023, 3059, and 3081 cm^{-1} corresponding to ν_{20b}, ν_{7b}, and ν_{20a}, respectively. To confirm that we are measuring two separate interfaces, we have also measured the SFG spectra before and after a short plasma treatment. As expected, the hidden PS/sapphire interface is not influenced by the plasma treatment, in contrast to the PS/air interface [12].

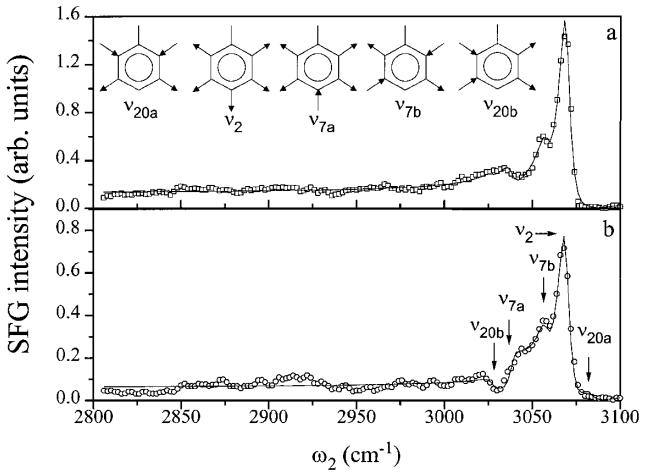

FIG. 2. The SFG spectra Ippp (squares) and Issp (circles) at an incident angle of 36°, corresponding to PS/air interface. The solid curves are the fit obtained using Eq. (1).

The differences in the PS/air and PS/sapphire spectra can be explained by the difference in orientation of the phenyl sidegroups at these interfaces. To quantitatively understand these differences, the SFG intensity can be expressed as a Lorentzian function [7]:

$$I(\mathrm{SFG}) \propto \left| \chi_{\mathrm{eff,NR}} + \sum_q \frac{A_q}{\omega_2 - \omega_q - i\Gamma_q} \right|^2, \qquad (1)$$

where A_q, Γ_q, and ω_q are the strength, damping constant, and angular frequency of a single resonant vibration, respectively. $\chi_{\mathrm{eff,NR}}$ is the nonresonant part of the signal. The solid curves in Figs. 2 and 3 correspond to the fits obtained using Eq. (1). The values A_q, Γ_q, and ω_q are summarized in Table I. Only the five aromatic C-H vibrational stretching modes were used to fit the PS/air data. For the PS/sapphire data an additional broad peak in the aliphatic region was used to capture the broad feature

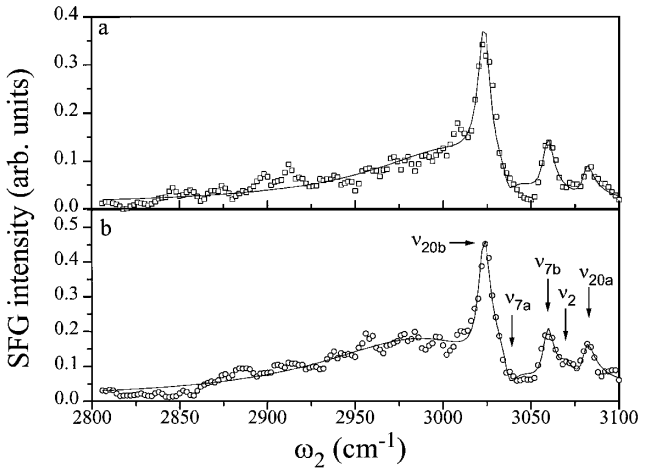

FIG. 3. The SFG spectra Ippp (squares) and Issp (circles) at an incident angle of 64°, corresponding to PS/sapphire interface. The solid curves are the fit obtained using Eq. (1).

TABLE I. A_q values found by fitting the PS/air and PS/sapphire SFG spectra for Issp and Ippp polarization (Figs. 2 and 3) to Eq. (1).

			PS/air			PS/sapphire		
q	Type	Γ_q (cm^{-1})	A_q (ssp)	A_q (ppp)	ω_q (cm^{-1})	A_q (ssp)	A_q (ppp)	ω_q (cm^{-1})
ν_{20a}	I	3.8	0.53	0.14	3082	0.57	0.52	3081
ν_2	I	3.9	3.07	4.56	3069	0.22	0.02	3069
ν_{7a}	I	4.1	−0.74	0.63	3038	−0.57	−0.37	3037
ν_{7b}	II	3.7	0.54	0.78	3058	0.76	0.72	3059
ν_{20b}	II	4.0	0.23	0.15	3027	1.33	1.31	3023

below 3000 cm^{-1}. From the fitting, it is apparent that the ν_2 mode dominates the Issp spectrum of the PS/air interface. Similar trends are seen in the Ippp spectrum of the PS/air interface. Conversely, analysis of the Issp and Ippp spectra of the PS/sapphire interface reveals that the spectra are dominated by the ν_{20b} and ν_{7b} modes.

The values of A_q can be used to determine the orientation of the phenyl sidegroups at the surface. The values of A_q are related to the hyperpolarizability tensor β, the number density, and the average orientation of the molecule of interest at the surface [7]. The five aromatic C-H vibrational stretching modes seen in the SFG spectra can be separated into two types of vibrations with very different hyperpolarizability tensors. Modes ν_2, ν_{7a}, and ν_{20a} belong to the first type of vibration, which we call type I. For type I vibrations, there are only two nonzero elements in β, β_{aac}, and β_{ccc}. The (a, b, c) molecular coordinates are shown as an inset in Fig. 4. For type II vibrations ν_{7b} and ν_{20b}, there are only two nonzero elements in β, $\beta_{caa} = \beta_{aca}$. In the case of PS surfaces, we assume that the projection of the phenyl molecular c axis into the plane of the surface (ϕ) and the twist of the molecular b axis out of the plane of the surface (ψ) are isotropically distributed. We believe this assumption to be valid because the PS films used in this study were annealed extensively above their glass transition temperature to remove any possible net orientation of polymer molecules in the plane of the surface. The orientation of the phenyl rings at the surface can then be described by the remaining tilt angle θ (see inset in Fig. 4). Qualitatively, if all of the aromatic rings were oriented with their c axes perpendicular to the plane of the surface ($\theta = 0°$), the Issp spectrum would contain only peaks corresponding to type I vibrations. If the phenyl rings were all lying flat in the plane of the surface ($\theta = 90°$), the Issp spectrum would contain no peaks. For all values of θ that lie between 0° and 90° and for any distribution of θ, the Issp spectrum will contain all five peaks.

An estimate of the tilt angle, θ, can be made by taking ratios of specific values from Table I. For example, in Issp polarization the ratio of $A_{q,\mathrm{II}}$ from a vibration of type II to $A_{q,\mathrm{I}}$ of a type I vibration is expressed by the following equation [13]:

$$R = \left|\frac{A_{q,\mathrm{II}}}{A_{q,\mathrm{I}}}\right| = \left|\left(\frac{\beta_{caa,\mathrm{II}}}{\beta_{aac,\mathrm{I}}}\right)\left(\frac{2(\langle\cos 3\theta\rangle - \langle\cos\theta\rangle)}{(7 + 2r)\langle\cos\theta\rangle + (1 - 2r)\langle\cos 3\theta\rangle}\right)\right|, \quad (2)$$

where $\beta_{caa,\mathrm{II}}$ is β_{caa} for the type II vibration, $\beta_{aac,\mathrm{I}}$ is β_{aac} for the type I vibration, and r is the ratio of β_{ccc}/β_{aac} for the type I vibration. Equation (2) predicts that the Issp intensity of the type II vibrational modes would increase relative to the type I vibrational modes as θ increases. From A_q values given in Table I, the $R_{\mathrm{PS/air}}$ are smaller than $R_{\mathrm{PS/sapphire}}$ for all vibrational modes, indicating that the phenyl rings are more tilted at the PS/sapphire interface than at the PS/air interface.

To determine the range of possible tilt angles, we need to know the ratio of $\beta_{caa,\mathrm{II}}/\beta_{aac,\mathrm{I}}$. Since $\beta_{caa,\mathrm{II}}/\beta_{aac,\mathrm{I}}$ is not known, we have rearranged Eq. (2) and plotted $(R\ \beta_{aac,7a}/\beta_{caa,20b})$ as a function of the tilt angle θ in Fig. 4 [$r\ (\nu_{7a}) = 0.25$ [14]]. The maximum value of $(R\ \beta_{aac,7a}/\beta_{caa,20b})$ in Fig. 4 is 1.33. Since $R_{\mathrm{PS/sapphire}} = 2.3$ for the PS/sapphire interface, this suggests that the ratio of $\beta_{caa,20b}/\beta_{aac,7a}$ is at least 1.7. The upper bound of $\beta_{caa,20b}/\beta_{aac,7a} \sim 2.5$ can be estimated based on infrared and Raman intensity. The shaded regions in Fig. 4 correspond to $(R\ \beta_{aac,7a}/\beta_{caa,20b})$ for PS/air (A) and PS/sapphire (B) interfaces taking $\beta_{caa,20b}/\beta_{aac,7a}$ between these two limits. For $\beta_{caa,20b}/\beta_{aac,7a} = 2.0$, the tilt angle ($\theta$) at the PS/air interface is 20° and the tilt angle at the PS/sapphire interface is 70° assuming all the phenyl rings are uniformly tilted at the surface. However, it is more likely that a distribution of tilt angles exists. The values of $(R\ \beta_{aac,7a}/\beta_{caa,20b})$ determined using a Gaussian distribution [15] and Eq. (2) are also shown in Fig. 4. Regardless of the inherent assumptions in estimating θ from R, it is evident that the aromatic rings are aligned almost parallel to the surface normal at the PS/air interface and almost perpendicular to the surface normal at the PS/sapphire interface.

The presence of strong phenyl peaks in comparison to methylene peaks in the SFG spectra at both the air and solid surface is surprising. Generally, one would expect the more hydrophobic methylene groups [16] to be present near the PS/air interface. However, our results suggest that either the microscopic susceptibilities, β's, for methylene

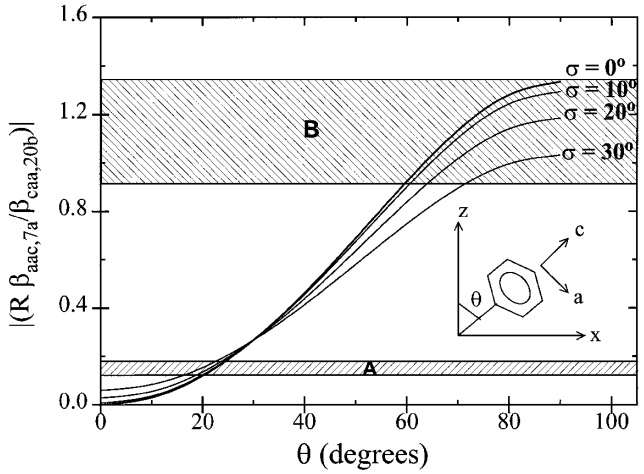

FIG. 4. $(R\ \beta_{aac,7a}/\beta_{caa,20b})$ as a function of tilt angle θ calculated using Eq. (2) and a Gaussian distribution of tilt angles [15]. Shaded regions *A* and *B* correspond to $(R\ \beta_{aac,7a}/\beta_{caa,20b})$ for PS/air and PS/sapphire interfaces assuming a range of $\beta_{caa,20b}/\beta_{aac,7a}$ from 1.7 to 2.5.

group are smaller in comparison to the phenyl ring or the methylene groups are not as well ordered at the interface. Since the strengths of methylene vibrations in both Raman and infrared spectra are as strong as the phenyl modes, the results suggest that the methylene groups are not as well ordered as the phenyl groups at the PS/air and PS/sapphire interface. Because the SFG results reported here do not include phase information, we cannot conclusively predict whether the phenyl rings at the air interface are pointing in or out with respect to the surface normal. Recent molecular dynamics simulation results on PS thin films in the melt have shown that the phenyl rings point outwards at the PS/air or vacuum interface [17]. These results are consistent with the physical picture obtained from the SFG measurements.

Finally, the measured SFG spectra at temperatures as high as 200 °C for both the PS/air and PS/sapphire interface, approximately 100 °C above the glass transition temperature of bulk PS, are nearly identical to those taken at room temperature. This suggests that the molecular surface structure of PS in the glassy state is very similar to the surface structure of the equilibrium liquid melt.

In summary, we have for the first time studied the molecular structure of the hidden polymer/solid interface. The aromatic C-H stretching modes are prominent in the PS/air and PS/sapphire SFG surface spectra. Also, the phenyl rings are oriented approximately parallel to the surface normal at the PS/air interface in comparison to nearly perpendicular to the surface normal at the PS/sapphire interface. In the future, extension of this work to polymer molecules of different architectures will provide a better understanding of the structure and dynamics of polymer melts in the vicinity of solid and polymer/polymer interfaces at a molecular level.

We acknowledge the NSF-CAREER grant (A. D.), Lord Corporation (A. D. S.), and The University of Akron (A. D.) for their financial support. Also we thank D. Peiffer (ExxonMobil) for many stimulating discussions and M. Varma-Nair (ExxonMobil) for a physical characterization of PS samples.

*Electronic address: alid@polymer.uakron.edu
†Electronic address: msyegan@erenj.com

[1] Special issue on Polymer Surfaces and Interfaces [MRS Bull. **21**, No. 1 (1996)]; G. T. Dee and B. B. Sauer, Adv. Phys. **47**, 161 (1998).
[2] R. J. Roe, Proc. Natl. Acad. Sci. U.S.A. **56**, 819 (1966); D. G. Legrand and G. L. Gaines, J. Colloid Interface Sci. **31**, 162 (1969); D. N. Theodorou, Macromolecules **22**, 4578 (1989).
[3] A. Silberberg, J. Colloid Interface Sci. **90**, 86 (1982); R. L. Jones, S. K. Kumar, D. L. Ho, R. M. Briber, and T. P. Russell, Nature (London) **400**, 146 (1999).
[4] A. Yethiraj, Phys. Rev. Lett. **74**, 2018 (1995).
[5] S. K. Kumar, A. Yethiraj, K. S. Schweizer, and F. A. M. Leermakers, J. Chem. Phys. **103**, 10 332 (1995); G. H. Fredrickson and D. T. Wu, Macromolecules **29**, 7919 (1996).
[6] J. G. Curro, J. D. Weinhold, J. D. McCoy, and A. Yethiraj, Comput. Theor. Polym. Sci. **8**, 159 (1998).
[7] Y. R. Shen, Nature (London) **337**, 519 (1989); X. Wei, X. Zhuang, S-C. Hong, T. Goto, and Y. R. Shen, Phys. Rev. Lett. **82**, 4256 (1999).
[8] S. R. Hatch, R. S. Polizzotti, S. Dougal, and P. J. Rabinowitz, J. Vac. Sci. Technol. A **11**, 2232 (1993); J. C. Conboy, J. L. Daschbach, and G. L. Richmond, J. Phys. Chem. **98**, 9688 (1994).
[9] M. S. Yeganeh, S. M. Dougal, R. S. Polizzotti, and P. Rabinowitz, Thin Solid Films **270**, 226 (1995).
[10] G. Varsanyi, *Vibrational Spectra of Benzene Derivatives* (Academic Press, New York, 1969).
[11] W. M. Sears, J. L. Hunt, and J. R. Stevens, J. Chem. Phys. **75**, 1589 (1981).
[12] D. Zhang, S. M. Dougal, and M. S. Yeganeh, Langmuir **16**, 4528 (2000).
[13] C. Hiroshe, N. Akamatsu, and K. Domen, Appl. Spectrosc. **46**, 1051 (1992); D. C. Duffy, P. B. Davies, and C. D. Bain, J. Phys. Chem. **99**, 15 241 (1995).
[14] The r for the ν_{7a} was determined using bond polarizability derivatives calculated by Whiffen [W. H. Whiffen, Proc. Phys. Soc. London Sect. A **69**, 375 (1956)] for C-H bonds.
[15] $P(\theta) = \frac{1}{\sigma\sqrt{\pi/2}} \exp(\frac{-2(\theta-\theta_0)^2}{\sigma^2})$.
[16] J. Israelachvili, *Intermolecular and Surface Forces* (Academic Press, San Diego, CA, 1997).
[17] J. H. Jang, K. S. Gautam, W. Mattice, M. S. Yeganeh, and A. Dhinojwala (to be published).